

Patterned Random Matrices: deviations from universality

Md. Sabir Ali¹, Shashi C. L. Srivastava^{1,2}

¹Variable Energy Cyclotron Centre, Kolkata 700064, India.

²Homi Bhabha National Institute, Training School Complex, Anushaktinagar, Mumbai - 400094, India

E-mail: shashi@vecc.gov.in

Abstract. We investigate the level spacing distribution for three ensembles of real symmetric matrices having additional structural constraint to reduce the number of independent entries to only $(n+1)/2$ in contrast to the $n(n+1)/2$ for a real symmetric matrix of size $n \times n$. We derive all the results analytically exactly for the 3×3 matrices and show that spacing distribution display a range of behaviour based on the structural constraint. The spacing distribution of the ensemble of reverse circulant matrices with additional zeros is found to fall slower than exponential for larger spacing while that of symmetric circulant matrices has poisson spacings. The palindromic symmetric toeplitz matrices on the other hand show level repulsion but the distribution is significantly different from Wigner. The behaviour of spacings for all the three ensembles clearly show the departure from universal result of Wigner distribution for real symmetric matrices. The deviation from universality continues in large n cases as well, which we study numerically.

Keywords: random matrices, level statistics

1. Introduction

Wigner conceptualized the random matrix theory (RMT) as a theory to explain fluctuation properties of the system, based solely on the symmetry properties of the Hamiltonian [1]. Since then RMT has been successfully applied in studies across the fields of Nuclear physics, condensed matter physics, mathematics[2, 3]. The Bohigas-Giannoni-Schmit (BGS) conjectured that fluctuation properties of spectrum of classically chaotic systems are described by the RMT ensembles dictated by the symmetry of the Hamiltonian[4] while Poisson distributed level spacings are characteristics of a generic integrable system [5]. Dyson’s three fold classification of the RMT ensembles based on the invariance of probability measure under the symmetry group have since then been generalized to 10 fold symmetry based classification [6, 7]. The universality of random matrix theory is attributed to such symmetry based approach. The universality is such a powerful tool that any deviation from it hints to some specific feature of the physical system.

Patterned matrices such as Toeplitz, Hankel, cyclic (circulant) matrices have attracted a lot of attention in mathematics and statistics community. The book [8] summarizes a lot of available results. The quantity of interest which has been looked most often are limiting spectral distributions (in physics literature commonly used term is eigenvalue density) and various moments [9, 10, 11, 12]. Circulant matrices are unarguably the most studied one in this family. This class of matrices have also been studied from the perspective of pseudo-Hermiticity, as well as constrained systems where constraints put on the matrices over and above the constraints put by symmetry requirements of the ensemble [13, 14, 15, 16, 17]. A number of physical scenarios where such a constraint can occur are discussed in [16].

In this paper we study three ensembles of real symmetric matrices, each having only $\frac{n+1}{2}$ number of independent elements in contrast to $\frac{n(n+1)}{2}$ independent elements of a real symmetric matrix constrained by orthogonal symmetry. We study the representative 3×3 matrices from each ensemble analytically exactly and indicate the results for larger dimensionality wherever possible. We compliment these studies numerically for not only 3×3 matrices but for general $n \times n$ dimensional matrices as well. The matrix elements are chosen to be independently Gaussian distributed subjected to the constraint imposed by the symmetry and structure of the matrix. Our quantity of interest here is the consecutive spacing distribution (also known as nearest neighbour spacing distribution) of the two independent eigenvalues for 3×3 case which we appropriately generalize to nearest neighbour spacing distribution of symmetry reduced spectrum in case of $n \times n$ dimensional matrices. These ensembles themselves find place in studying the systems for which Hamiltonian is translationally invariant and has coupling matrices as cyclic matrix [18], a particle doing the Markovian walk on a circle [19], or the problem of studying Ohm’s law on a disk [20]. We define and study the variation of ensemble of reverse cyclic, symmetric cyclic and palindromic symmetric Toeplitz matrices in Section 2, 3 and 4. The details of spacing distribution calculations are presented for

3×3 matrices and contrasting results are shown for the three ensembles despite them being the symmetric matrix with exactly two independent elements. The numerical results for $n \times n$ dimensional matrices of the respective class are also presented and similarity/deviation from their 3×3 analogue is discussed.

2. Random reverse cyclic matrices with additional zeros

Consider an ensemble of reverse cyclic (RC) matrices, drawn from a Wishart distribution,

$$P(H) \sim \exp(-A\text{Tr}(H^\dagger H)), \quad (1)$$

with A as normalization constant. Let us start with the simplest case, namely an ensemble of 3×3 reverse cyclic matrices with one entry $c = 0$ ‡

$$H = \begin{pmatrix} a & b & c \\ b & c & a \\ c & a & b \end{pmatrix}. \quad (2)$$

Using (1), the joint probability distribution function (JPDF) in matrix space will be given by,

$$P(a, b, c) = \left(\frac{3A}{\pi}\right) \exp[-3A(a^2 + b^2 + c^2)]\delta(c). \quad (3)$$

Karner *et al.* [21] have shown that the eigen-decomposition for an odd-dimensional reverse cyclic matrix is given by

$$H = F^\dagger \begin{pmatrix} 1 & 0 \\ 0 & R \end{pmatrix} \Lambda \begin{pmatrix} 1 & 0 \\ 0 & R^\dagger \end{pmatrix} F \quad (4)$$

$$\Lambda = (E_1, |E_2|, \dots, |E_{(n-1)/2}|, -|E_{(n-1)/2}|, \dots, -|E_2|),$$

where F is Fourier matrix. For the 3×3 case, the explicit form of R is

$$R = \begin{pmatrix} \frac{1}{\sqrt{2}} \exp(-i\theta/2) & \frac{i}{\sqrt{2}} \exp(-i\theta/2) \\ \frac{1}{\sqrt{2}} \exp(i\theta/2) & -\frac{i}{\sqrt{2}} \exp(i\theta/2) \end{pmatrix}. \quad (5)$$

It takes a simple algebra then to show that

$$a = \frac{1}{3}(E_1 + 2|E_2| \cos \theta)$$

$$b = \frac{1}{3} \left(E_1 - |E_2| \left(\cos \theta + \sqrt{3} \sin \theta \right) \right) \quad (6)$$

$$c = \frac{1}{3} \left(E_1 - |E_2| \left(\cos \theta - \sqrt{3} \sin \theta \right) \right).$$

Using (6) in (3), we can find the JPDF for eigenvalues and an independent parameter θ coming from the eigenvector. Note that in H , the independent parameters are three

‡ This ensemble of size $n \times n$ matrices can be constructed by choosing first $(n+1)/2$ from independent Gaussian distributions while rest $(n-1)/2$ entries are set to zero.

in number, namely a, b and c ; while in the eigen-decomposition, we have E_1, E_2, θ . The Jacobian for the transformation (6) is given by $\frac{2|E_2|}{3\sqrt{3}}$. The JPDF for eigenvalues is

$$P(E_1, |E_2|, \theta) = \frac{2|E_2|}{3\sqrt{3}} \left(\frac{3A}{\pi} \right) \exp[-A(E_1^2 + 2E_2^2)] \delta \left[\frac{1}{3} \left(E_1 - 2|E_2| \sin \left(\frac{\pi}{6} - \theta \right) \right) \right]$$

where $E_1 \in (-\infty, \infty), |E_2| \in [0, \infty), \theta \in [0, 2\pi)$.

Notice that the domain of $|E_2|$ is $[0, \infty)$, and that the function on the right hand side is an even function of E_2 . Using the following identity for δ -function,

$$\delta(f(\theta)) = \sum_n \frac{\delta(\theta - \theta_n)}{f'(\theta_n)},$$

and the fact that between $[0, 2\pi)$, we will have two roots, we can rewrite the JPDF after an integration over θ in the following form,

$$P(E_1, E_2) = \frac{2|E_2|}{3\sqrt{3}} \left(\frac{3A}{\pi} \right) \exp(-A(E_1^2 + 2E_2^2)) \int_0^{2\pi} \sum_n \frac{\delta(\theta - \theta_n)}{|f'(\theta_n)|} d\theta \quad (7)$$

The zeros of the delta function argument occur at,

$$\theta_1 = \frac{1}{6} \left[\pi - 6 \sin^{-1} \left(\frac{E_1}{2|E_2|} \right) \right], \quad \theta_2 = \frac{1}{6} \left[\pi - 6 \left(\pi - \sin^{-1} \left(\frac{E_1}{2|E_2|} \right) \right) \right]$$

and the derivative of the function evaluated at these values are,

$$|f'(\theta_1)| = \frac{1}{3} \sqrt{4|E_2|^2 - E_1^2}, \quad |f'(\theta_2)| = \frac{1}{3} \sqrt{4|E_2|^2 - E_1^2}.$$

Using these, (7) becomes,

$$P(E_1, E_2) = \begin{cases} \frac{2|E_2|}{3\sqrt{3}} \left(\frac{3A}{\pi} \right) \exp(-A(E_1^2 + 2E_2^2)) \frac{6}{\sqrt{4|E_2|^2 - E_1^2}} & \left| \frac{E_1}{2|E_2|} \right| \leq 1. \\ 0 & \text{otherwise.} \end{cases} \quad (8)$$

The density distribution of E_1 which we will refer as trivial eigenvalue being the sum of all the elements in the first row, can be found out to be,

$$\begin{aligned} P(E_1) &= \int P(E_1, E_2) dE_2 \\ &= \int_{\frac{|E_1|}{2}}^{\infty} \frac{4|E_2|}{\sqrt{3}\sqrt{4|E_2|^2 - E_1^2}} \left(\frac{3A}{\pi} \right) \exp(-A(E_1^2 + 2E_2^2)) dE_2 \\ &= \sqrt{\frac{3A}{2\pi}} e^{-\frac{3}{2}AE_1^2}, \end{aligned} \quad (9)$$

while density distribution of E_2 which we will refer as non-trivial positive eigenvalue is,

$$\begin{aligned} P(E_2) &= \int P(E_1, E_2) dE_1 \\ &= \int_{-2E_2}^{2E_2} \frac{4|E_2|}{\sqrt{3}\sqrt{4|E_2|^2 - E_1^2}} \left(\frac{3A}{\pi} \right) \exp(-A(E_1^2 + 2E_2^2)) dE_1 \\ &= 4\sqrt{3}AE_2 e^{-4AE_2^2} I_0(2AE_2^2). \end{aligned} \quad (10)$$

The free parameter A is fixed by setting the mean energy $\langle E_2 \rangle$ as 1. Such a distribution is compared with numerics in Fig.1. The density of trivial eigenvalue for the n -dimensional

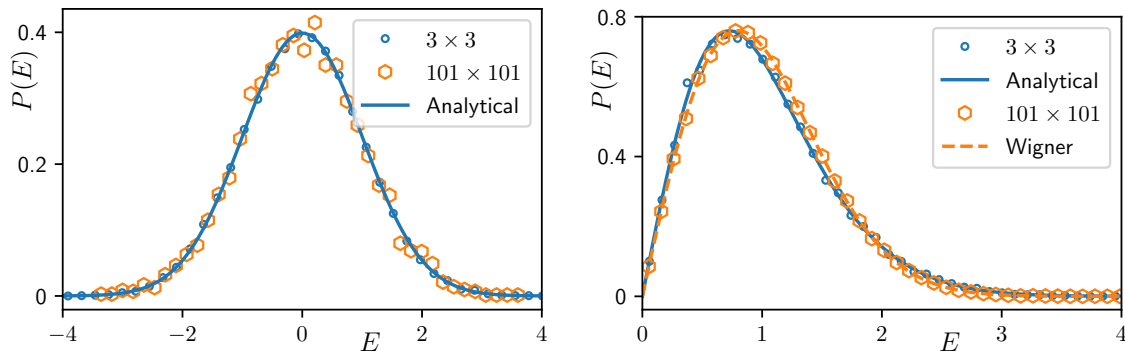


Figure 1. (Left) For 3×3 reverse-circulant matrices with $c = 0$, numerical density distribution of the trivial eigenvalue with sample size 50000 is shown by blue open circle. The result agrees well with the analytical prediction obtained in Eq. 9 (represented by the solid blue line). Orange hexagons represent the numerical density of trivial eigenvalue for 101×101 matrices of this class with sample size 4000. (Right) For 3×3 reverse-circulant matrices with $c = 0$ (represented by blue open circles) as well as for 101×101 matrices of this class (represented by orange hexagons), numerical density distribution of the non-trivial positive eigenvalue with sample size 50000 and 4000 respectively. The result for 3×3 agrees well with the analytical prediction (represented by solid blue line) obtained in Eq. 10 while density for 101×101 goes to Wigner distribution (represented by orange dashed line).

matrices remains Gaussian while density of non-trivial (positive) eigenvalues deviates from analytical result obtained in Eq. 10 and transits to Wigner distribution. This is in agreement with the result of random reverse circulant matrices with n -independent elements [15]. These results are clearly borne out from numerical data presented in Fig. 1. The fluctuation seen for trivial eigenvalue density in the case of 101×101 is due to smaller sample size of 4000 considered here as for each sample we obtain only one trivial eigenvalue and fifty non-trivial positive eigenvalue.

2.1. Spacing distribution

Let's define the spacing, s between trivial eigenvalue E_1 and the positive non-trivial eigenvalue E_2 as $s = |E_1 - E_2|$. Then the distribution of s is defined using JPDF (8) as,

$$P(s) = \int P(E_1, E_2) \delta(s - |E_1 - E_2|) dE_1 dE_2 \quad (11)$$

We can rewrite equation (11) in terms of eigenvalues explicitly using equation (8) and after applying proper limits one gets,

$$\begin{aligned}
 P(s) &= \frac{4\sqrt{3}A}{\pi} \int_0^\infty E_2 \exp[-2Ae_2^2] \int_{-2E_2}^{2E_2} \frac{\exp[-Ae_1^2]}{\sqrt{4E_2^2 - E_1^2}} \delta(s - |E_1 - E_2|) dE_1 dE_2 \\
 &= k \int_0^\infty E_2 \exp[-2Ae_2^2] I(E_2) dE_2
 \end{aligned} \tag{12}$$

where $k = \frac{4\sqrt{3}A}{\pi}$ and $I(E_2)$ is defined as,

$$I(E_2) = \int_{-2E_2}^{2E_2} \frac{\exp[-AE_1^2]}{\sqrt{4E_2^2 - E_1^2}} \delta(s - |E_1 - E_2|) dE_1. \tag{13}$$

Taking care of the domain of JPDF of eigenvalues, equation (13) can be broken into two parts with respective limits as shown below,

$$\begin{aligned}
 I(E_2) &= \int_{-2E_2}^{E_2} \frac{\exp[-AE_1^2]}{\sqrt{4E_2^2 - E_1^2}} \delta(s - (E_2 - E_1)) dE_1 + \int_{E_2}^{2E_2} \frac{\exp[-AE_1^2]}{\sqrt{4E_2^2 - E_1^2}} \delta(s - (E_1 - E_2)) dE_1 \\
 &= I_1 + I_2
 \end{aligned} \tag{14}$$

I_1 and I_2 can be evaluated separately under certain conditions which are stated below,

$$\begin{aligned}
 I_1 &= \begin{cases} \frac{\exp[-A(e_2-s)^2]}{\sqrt{4e_2^2 - (e_2-s)^2}} & \text{for } e_2 \geq \frac{s}{3} \text{ and } s \geq 0, \\ 0 & \text{otherwise} \end{cases} \\
 I_2 &= \begin{cases} \frac{\exp[-A(e_2+s)^2]}{\sqrt{4e_2^2 - (e_2+s)^2}} & \text{for } e_2 \geq s \text{ and } s \geq 0, \\ 0 & \text{otherwise} \end{cases}.
 \end{aligned} \tag{15}$$

Utilizing (15), the spacing distribution is,

$$P(s) = \frac{4A}{\pi} \exp\left[-\frac{4A}{6}s^2\right] \left[\int_0^\infty \frac{(x + \frac{s}{3}) \exp[-3Ax^2]}{\sqrt{x(x + \frac{4s}{3})}} dx + \int_{\frac{4s}{3}}^\infty \frac{(x - \frac{s}{3}) \exp[-3Ax^2]}{\sqrt{x(x - \frac{4s}{3})}} dx \right] \tag{16}$$

For $s = 0$ one can show from eq. (16) that,

$$P(s \rightarrow 0) = \frac{4}{\sqrt{3}} \sqrt{\frac{A}{\pi}}. \tag{17}$$

The probability distribution of spacing deviates from Poisson and Wigner distribution expected from orthogonal symmetry. Such deviations from universal results are characteristic feature of patterned random matrices. The behaviour of $P(s)$ obtained analytically in (16) is compared against the numerical calculation in Fig. 2. The agreement between the two is very good.

To separate the role played by ‘‘hard’’ constraint of putting $c = 0$ from the symmetry, we numerically studied the distribution of spacing between trivial eigenvalue

and non-trivial positive eigenvalue by choosing c as a normal distributed random number with mean 0 and finite variance. Note that variance approaching to zero is equivalent to $c \rightarrow 0$. The distribution goes from Eq. 16 to semi-Gaussian distribution as we increase the variance. This transition is clearly visible in Fig. 2 (Left Panel). For comparable variances of all the three elements, the matrix is in random reverse circulant matrix class with all the three independent elements and the distribution comes out to be semi-Gaussian expectedly as derived in [15] for random reverse circulant matrices. Moreover, we will see that constraint of putting the two elements namely b and c equal also yields the semi-Gaussian as obtained in Eq. 23. This clearly shows that hard constraint of putting $c = 0$ fundamentally change the behaviour of spacings. Such behaviour when hard constraints affect the spacing distribution has been studied in the case of random banded matrices where level repulsion develops logarithmic singularity due to constraint [22].

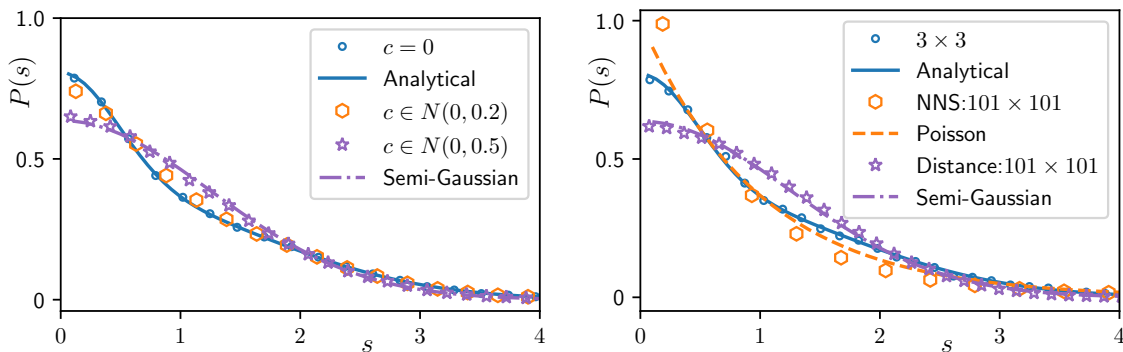


Figure 2. (Left) Plot of transition in $P(s)$ for 3×3 reverse-circulant matrices as we “soften” the constraint on c from 0 to a Gaussian distributed random number with mean 0 and finite variance. Blue open circles represent the behaviour for zero variance *i.e.* $c=0$. Orange hexagons and purple stars represent the behaviour for variances $\sigma = 0.2$ and $\sigma = 0.5$ respectively. In both the panels, solid blue line represents the spacing distribution calculated analytically (16) and the purple dash-dot line represents semi-Gaussian curve (23). (Right) Plot of probability distribution function (PDF) of spacing between trivial eigenvalue and non-trivial positive eigenvalue for 3×3 case (represented by blue open circles) along with PDF of distance between trivial eigenvalue to each of the positive non-trivial eigenvalue for 101×101 size matrices (represented by purple stars). The nearest neighbour spacing distribution of positive eigenvalues is also plotted for 101×101 which tends towards Poisson distribution (represented by orange hexagons). Orange dashed line represents a Poisson distribution. In all the plots, marker symbols are used for numerically obtained data, while lines are respective analytical results.

We extend our studies to large matrix sizes numerically. The spectrum of these constrained random reverse circulant matrices has always one eigenvalue as the sum of the first row elements, and rest eigenvalues come in \pm pair. As we are interested in symmetry reduced spectrum in spacing distribution, we leave out all the negative eigenvalues from the \pm pair. We study two quantities (i) distance between trivial

eigenvalue to each of the positive non-trivial eigenvalue and (ii) the nearest neighbour spacing (NNS) between non-trivial positive eigenvalues. It turns out that in large n (dimensionality of matrix) limit the probability distribution of distance between trivial to positive non-trivial eigenvalue becomes semi-Gaussian, a result obtained for the case of unconstrained random reverse circulant matrices. The NNS on the other hand tend to become Poisson distribution as seen in Fig. 2 (Right Panel). Clearly reducing the independent elements from n to $(n + 1)/2$ is not enough in the large n limit to affect the spacing distribution to deviate from random reverse circulant matrices. Having said that, the spacing distribution is far from Wigner distribution expected from real symmetric matrices.

3. Symmetric circulant matrices

Symmetric circulant matrices naturally occur as a coupling matrix whenever Hamiltonian of the system is translationally invariant along with the fact that it is hermitian [18]. In a classical setting of studying Ohm's law on a disk, the Ohm's matrix relating the vectors of voltages and currents is symmetric circulant[20]. Consider an ensemble of such symmetric circulant matrices, drawn from a Wishart distribution. Let us start again with the simplest case, namely an ensemble of 3×3 cyclic (circulant) matrices with additional constraint $b = c$,

$$H = \begin{pmatrix} a & b & c \\ c & a & b \\ b & c & a \end{pmatrix}. \quad (18)$$

The $n \times n$ generalization of the symmetric matrix is obtained easily by setting the first row element of a circulant matrix such that $a_{n-i} = a_i, i = 1, \dots, (n - 1)$. Using (1), the JPDF in matrix space will be given by,

$$P(a, b, c) = \left(\frac{3\sqrt{2}A}{\pi} \right) \exp[-3A(a^2 + b^2 + c^2)]\delta(b - c). \quad (19)$$

The eigenvalues of this symmetric circulant matrix is given by,

$$\begin{bmatrix} E_1 \\ E_2 \end{bmatrix} = \begin{bmatrix} 1 & 2 \\ 1 & 2 \cos \frac{2\pi}{3} \end{bmatrix} \begin{bmatrix} a \\ b \end{bmatrix}.$$

Using this relation along with the fact that eigenfunctions are columns of discrete Fourier matrix, the joint probability distribution of eigenvalues can straightforwardly be written as,

$$P(E_1, E_2) = \frac{\sqrt{2}A}{\pi} \exp(-A(E_1^2 + 2E_2^2)). \quad (20)$$

Note that number of independent eigenvalues are only two, the third is additive inverse equal to E_2 . Also H commutes with a parity like operator η defined as,

$$\eta = \begin{bmatrix} 1 & 0 & 0 \\ 0 & 0 & 1 \\ 0 & 1 & 0 \end{bmatrix} \quad \text{with} \quad \eta^2 = \begin{bmatrix} 1 & 0 & 0 \\ 0 & 1 & 0 \\ 0 & 0 & 1 \end{bmatrix}.$$

This pattern generalizes for $n \times n$ matrices as well. Due to this fact, the spectrum of the matrix separates into two, one with even parity while the other with odd parity. The two eigenvalues considered here correspond to even parity sector. This information is important for the calculation of spacing distribution for which we need symmetry reduced spectrum. For spacing distribution, we consider only non-trivial eigenvalues. The ordering of the eigenvalues before the calculation of nearest neighbour distribution is simple in this case namely $E_2 = E_1 \pm s$. The spacing distribution then is defined as,

$$P(s) = \int p(E_1, E_1 + s)dE_1 + \int p(E_1, E_1 - s)dE_1 \quad (21)$$

It is straightforward to evaluate the two Gaussian integration, which yields the spacing distribution as,

$$P(s) = 2\sqrt{\frac{2}{3\pi}}\sqrt{A}e^{-\frac{1}{3}(2As^2)}. \quad (22)$$

After scaling the spacing in such a way that mean spacing becomes one, distribution of scaled spacing is,

$$P(\tilde{s}) = \frac{2}{\pi}e^{-\frac{\tilde{s}^2}{\pi}}. \quad (23)$$

This is the Poisson equivalent for two eigenvalue case for spacing distribution [23]. The $N \times N$ generalization of this spacing distribution is expected to be Poisson. Like in constrained reverse circulant matrices, we plot the probability distribution of distance between trivial eigenvalue and rest of the even parity eigenvalue as well as the nearest neighbour distribution for even parity spectrum of 101×101 size matrices from this ensemble in Fig. 3. The distance distribution remains semi-Gaussian like 3×3 case, while NNS approaches to Poisson distribution.

A contrasting point to note here is that spacing distribution comes out to be very different despite the two ensembles containing real symmetric matrices and exactly the same number of independent matrix elements for 3×3 matrix, but differences does not survive the large n limit.

4. Palindromic symmetric Toeplitz (PST) matrices

The third ensemble is of palindromic symmetric Toeplitz matrices which are studied again mainly in mathematics literature for the limiting spectral distributions of eigenvalues [24, 25, 26, 12]. The spacing distribution has been conjectured to be Poisson

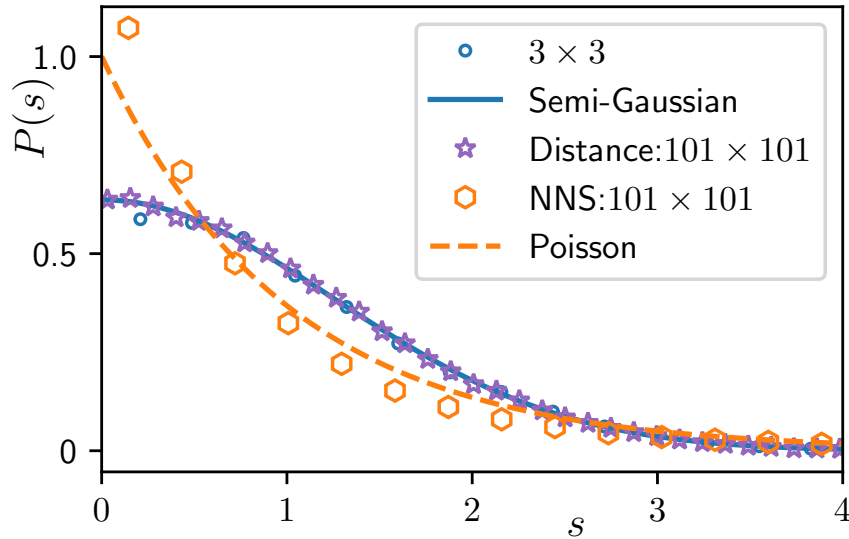


Figure 3. Plot of probability distribution function (PDF) of spacing between even parity eigenvalues for 3×3 case (represented by blue open circles) along with PDF of distance between trivial eigenvalue to each of non-trivial even parity eigenvalues for 101×101 size matrices (represented by purple stars). The nearest neighbour spacing distribution of even parity symmetry eigenvalues is also plotted for 101×101 which tends towards Poisson distribution (represented by orange hexagons). Solid blue line represents a semi-Gaussian function (23) and the orange dashed line represents a Poisson distribution. Different marker symbols are used for numerically obtained data, while lines are used for respective analytical/functional form.

in [26]. Let's again start with the simplest case of 3×3 matrices.

$$H = \begin{pmatrix} a & b & a \\ b & a & b \\ a & b & a \end{pmatrix}. \quad (24)$$

The JPDF of the matrix elements when matrices are taken from Wishart distribution are written as,

$$P(a, b) = \frac{2\sqrt{5}A}{\pi} \exp[-A(5a^2 + 4b^2)]. \quad (25)$$

The eigenvalues (E_1 , E_2 and E_3) of 3×3 PST matrices are given by,

$$\begin{aligned} E_1 &= 0 \\ E_2 &= \frac{1}{2}(3a + \sqrt{a^2 + 8b^2}) \\ E_3 &= \frac{1}{2}(3a - \sqrt{a^2 + 8b^2}) \end{aligned} \quad (26)$$

Finally, using equations (25), (26) and computing the jacobian we arrive at,

$$P(E_1 = 0, E_2, E_3) = \frac{\sqrt{5}A}{2\pi} \frac{|E_3 - E_2|}{\sqrt{(E_3 - E_2)^2 - \frac{1}{2}E_2E_3}} \exp[-A(E_2^2 + E_3^2)] \quad (27)$$

The spacing between the eigenvalues E_2 and E_3 in terms of matrix elements is,

$$s = (E_3 - E_2) = \sqrt{a^2 + 8b^2}. \quad (28)$$

Using substitution $a = r \cos \theta$ and $\sqrt{8}b = r \sin \theta$, the spacing distribution therefore can be calculated as,

$$\begin{aligned} P(s) &= \frac{2\sqrt{5}A}{\pi} \int \exp[-A(5r^2 - \frac{9}{2}r^2 \sin^2 \theta)] \delta(s - r) \frac{r}{\sqrt{8}} da db \\ &= \sqrt{10}A s I_0\left(\frac{9}{4}As^2\right) e^{-\frac{11}{4}As^2}. \end{aligned} \quad (29)$$

In rescaled variable $x = s/\bar{s}$ the distribution obtained in (29) transforms to,

$$P(x) = \frac{2\sqrt{10}E\left(\frac{9}{10}\right)^2}{\pi} x e^{-\frac{11E\left(\frac{9}{10}\right)^2}{2\pi}x^2} I_0\left(\frac{9x^2E\left(\frac{9}{10}\right)^2}{2\pi}\right) \quad (30)$$

where $E\left(\frac{9}{10}\right)$ is the complete Elliptic integral defined as, $\int_0^{\pi/2} \sqrt{1 - m \sin^2 \theta} d\theta$ and $I_0(z)$ is the modified Bessel function of the first kind of order zero. The spacing distribution is plotted in Fig. (4) and compared with the numerical distribution. We can clearly

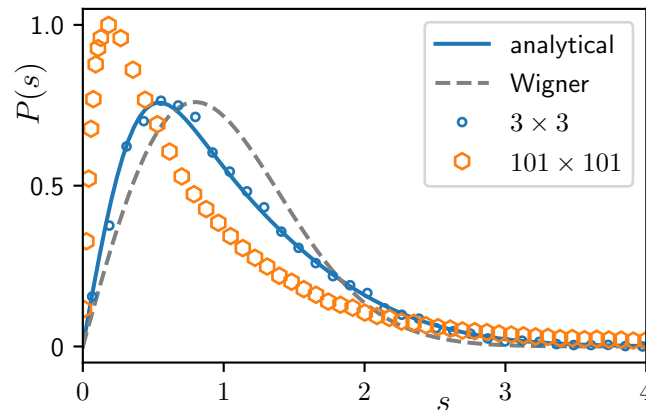


Figure 4. Numerically computed normalized spacing distribution $P(s)$ (represented with blue open circles) for 3×3 palindromic symmetric Toeplitz matrices is plotted along with the analytical result (30) (represented by the solid blue line). The Wigner distribution (represented by dashed line) is plotted to show the extent of deviation. The nearest neighbour spacing distribution for non-zero even-parity eigenvalues for 101×101 size matrices are plotted which shows level repulsion (represented by the orange hexagons). The 7000 samples of 101×101 size matrices are utilized to obtain the numerical distribution.

see the level repulsion in this ensemble but the form of which is different from the Wigner distribution. The extent of deviation from this universal result of Wigner is quite pronounced in Fig. (4).

We further study the spacing distribution for large n -dimensional matrices of this class numerically. Like symmetric circulant case, the palindromic symmetric Toeplitz matrices commutes with a parity like operator defined as,

$$\sigma = \begin{bmatrix} 0 & 0 & 1 \\ 0 & 1 & 0 \\ 1 & 0 & 0 \end{bmatrix} \quad \text{with } \sigma^2 = \begin{bmatrix} 1 & 0 & 0 \\ 0 & 1 & 0 \\ 0 & 0 & 1 \end{bmatrix}$$

This implies that spectrum is divided into two parts, one with even parity and the other with odd parity. For all the odd-dimension matrix of this class, one eigenvalue will always be zero. Therefore, we study the nearest neighbour distribution of non-zero even parity eigenvalues. The numerically obtained probability distribution function with average spacing of one is plotted in the Fig. 4. This distribution though shows level repulsion, is very different from Wigner distribution. The importance of symmetry reduced spectrum to study the spacings can not be overemphasized as one would obtain the Poisson distribution in place of level repulsion due to mixing of two parity sectors of the spectrum.

5. Summary and discussion

In this paper, we have studied patterned random matrices which are real symmetric with only $(n + 1)/2$ independent entries in contrast to $n(n + 1)/2$ independent entries allowed for real symmetric matrices. We mainly focussed on the calculation of spacing distribution and restricted our attention to 3×3 matrices to derive all the distributions analytically. We have analytically shown and numerically verified that spacing distributions come out to be very different ranging from a heavy tailed one for reverse circulant matrices with additional zeros to level repulsion coming from the additional structural constraint put on these matrices. The $n \times n$ generalizations of symmetric circulant is fairly simple and spacing becomes Poisson distributed, but the similar level of analytical understanding is beyond the reach of methods used in this work. The biggest bottleneck presents itself in terms of absence of eigenvalue formulae in terms of matrix elements for PST ensembles. Therefore, we studied the large dimensional generalizations numerically and have shown that in large n -limit, constrained reverse circulant matrices and symmetric circulant matrices approach to the same spacing distribution which in this case is Poisson and not Wigner as expected for Gaussian orthogonal ensemble. The palindromic symmetric toeplitz matrices on the other hand despite having exactly same number of elements as the previous two cases display level repulsion. The distribution itself is different from Wigner distribution. To summarize, the patterned random matrices continue to surprise in terms of the behaviour of spacing distribution away from universality despite having the same symmetry class and equal number of independent elements.

References

- [1] Wigner E P 1957 Statistical properties of real symmetric matrices with many dimensions *Can. Math. Congr. Proc.* 174
- [2] Guhr T, Müller-Groeling A and Weidenmüller H A 1998 Random-matrix theories in quantum physics: common concepts *Phys. Rep.* **299** 189–425
- [3] Fyodorov Y 2011 Random matrix theory *Scholarpedia* **6** 9886
- [4] Bohigas O, Giannoni M J and Schmit C 1984 Characterization of chaotic quantum spectra and universality of level fluctuation laws *Phys. Rev. Lett.* **52** 1–4
- [5] Berry M V and Tabor M 1977 Level clustering in the regular spectrum *Proc. R. Soc. Lon. A* **356** 375–394
- [6] Dyson F J 1962 The threefold way. Algebraic structure of symmetry groups and ensembles in quantum mechanics *J. Math. Phys.* **3** 1199–1215 0022-2488
- [7] Altland A and Zirnbauer M R 1997 Nonstandard symmetry classes in mesoscopic normal-superconducting hybrid structures *Phys. Rev. B* **55** 1142–1161
- [8] Bose A 2018 *Patterned random matrices* (Chapman and Hall/CRC)
- [9] Bose A, Saha K and Sen P 2021 Some patterned matrices with independent entries *Random Matrices: Theory and Applications* **10** 2150030
- [10] Bose A, Saha K and Sen P 2022 Erratum: Some patterned matrices with independent entries *Random Matrices: Theory and Applications* **11** 2292001
- [11] Adhikari K and Saha K 2017 Fluctuations of eigenvalues of patterned random matrices *Journal of Mathematical Physics* **58** 063301
- [12] Blackwell K, Borade N, Bose A, VI C D, Luntzlar N, Ma R, Miller S J, Mukherjee S S, Wang M and Xu W 2021 Distribution of eigenvalues of matrix ensembles arising from wigner and palindromic toeplitz blocks
- [13] Jain S R and Srivastava S C L 2008 Random cyclic matrices *Phys. Rev. E* **78** 036213
- [14] Jain S R and Srivastava S C L 2009 Random matrix theory for pseudo-Hermitian systems: Cyclic blocks *Pramana-J. Phys.* **73** 989
- [15] Srivastava S C L and Jain S R 2012 Random reverse-cyclic matrices and screened harmonic oscillator *Phys. Rev. E* **85**(4) 041143
- [16] Shukla P and Sadhukhan S 2015 Random matrix ensembles with column/row constraints: I *J. Phys. A - Math. Theor.* **48** 415002
- [17] Sadhukhan S and Shukla P 2015 Random matrix ensembles with column/row constraints: II *J. Phys. A - Math. Theor.* **48** 415003
- [18] Gluza M, Eisert J and Farrelly T 2019 Equilibration towards generalized Gibbs ensembles in non-interacting theories *SciPost Phys.* **7**(3) 38
- [19] Manikandan K, Srivastava S C L and Jain S R 2011 Biased random walks on a disordered one-dimensional lattice *Phys. Lett. A* **375** 368
- [20] Demidenko E 2017 Applications of Symmetric Circulant Matrices to Isotropic Markov Chain Models and Electrical Impedance Tomography *Adv. in Pure Math.* **7** 188
- [21] Karner H, Schneid J and Ueberhuber C W 2003 Spectral decomposition of real circulant matrices *Linear Algebra Appl.* **367** 301
- [22] Molinari L and Sokolov V V 1989 Level repulsion for band 3 times 3 random matrices *Journal of Physics A: Mathematical and General* **22** L999
- [23] Berry M V and Shukla P 2009 Spacing distributions for real symmetric 2 times 2 generalized gaussian ensembles *J. Phys. A - Math. Theor.* **42** 485102
- [24] Bose A, Chatterjee S and Gangopadhyay S Limiting spectral distribution of large dimensional random matrices *J. Indian Statist. Assoc.* **41** 221 – 259
- [25] Bryc W, Dembo A and Jiang T 2006 Spectral measure of large random Hankel, Markov and Toeplitz matrices *The Annals of Probability* **34** 1 – 38
- [26] Massey A, Miller S J and Sinsheimer J 2007 Distribution of eigenvalues of real symmetric

palindromic toeplitz matrices and circulant matrices *Journal of Theoretical Probability* **20** 637–662 1572-9230